Selinger, Julian; Islam, M. Tauhidul; Abbas, Qamar; Schaubeder, Jana B.; Zoder, Janis; Bakhshi, Adelheid; Bauer, Wolfgang; Hummel, Michael; Spirk, Stefan

Form-stable, crosslinked cellulose-based paper separators for charge storage applications

Published in:
Carbohydrate Polymers

DOI:
10.1016/j.carbpol.2024.122354

Published: 01/11/2024

Document Version
Publisher's PDF, also known as Version of record

Please cite the original version:
Selinger, J., Islam, M. T., Abbas, Q., Schaubeder, J. B., Zoder, J., Bakhshi, A., Bauer, W., Hummel, M., & Spirk, S. (2024). Form-stable, crosslinked cellulose-based paper separators for charge storage applications. *Carbohydrate Polymers*, *343*, Article 122354. https://doi.org/10.1016/j.carbpol.2024.122354

Carbohydrate Polymers 343 (2024) 122354

Contents lists available at ScienceDirect

Carbohydrate Polymers

journal homepage: www.elsevier.com/locate/carbpol

Form-stable, crosslinked cellulose-based paper separators for charge storage applications

Julian Selinger [a,b], M. Tauhidul Islam [c], Qamar Abbas [c,d], Jana B. Schaubeder [a], Janis Zoder [a], Adelheid Bakhshi [a], Wolfgang Bauer [a], Michael Hummel [b], Stefan Spirk [a,e,*]

[a] *Institute of Bioproducts and Paper Technology, Graz University of Technology, Inffeldgasse 23, 8010 Graz, Austria*
[b] *Department of Bioproducts and Biosystems, Aalto University, Vuorimiehentie 1, FI-00076 Aalto, Finland*
[c] *Institute for Chemistry and Technology of Materials, Graz University of Technology, Stremayrgasse 9, 8010 Graz, Austria*
[d] *Institute of Chemistry and Technical Chemistry, Faculty of Chemical Technology, Poznan University of Technology, Berdychowo 4, 60965 Poznan, Poland*
[e] *Ecolyte GmbH, Inffeldgasse 21B, 8010 Graz, Austria*

ARTICLE INFO

Keywords:
Separator design
Microfibrillated cellulose
Crosslinking
Energy storage
Paper-making

ABSTRACT

In the quest for greener and more efficient energy storage solutions, the exploration and utilization of renewable raw materials is essential. In this context, cellulose-derived separators play a central role in enhancing the performance of green energy storage devices. However, these often exhibit disadvantageous porosity and limited wet strength. Here, we demonstrate a facile approach to tailor thickness (ca. 40 µm), air permeability (0.1–200 $cm^3\ s^{-1}$), and mechanical properties of separators by integration of up to 50 wt% microfibrillated cellulose (MFC) into paper sheets. While the MFC enhanced the formation of dense networks, these separators show a poor dimensional stability (folding and creasing) concomitant with a low strength under wet conditions, crucial for assembly and operation. Crosslinking with 1,2,3,4-butanetetracarboxylic acid (BTCA) however, led to an increase in wet strength by up to 6700 % while ensuring dimensional stability. The electrochemical performance, evaluated by impedance spectroscopy and galvanostatic cycling (7500 repetitions) showed comparable results as commercially available glass and polypropylene separators in terms of ion diffusion, charge-discharge rate performance, Ohmic loss and capacitance retention %. The approach demonstrates that disadvantages of paper-based separators in terms of dimensional stability and wet strength can be overcome by a paper technological approach using crosslinking strategies.

1. Introduction

Renewable materials are important resources to improve the sustainability and efficiency of energy storage systems such as batteries and supercapacitors (Schlemmer et al., 2021). They have been identified by the research roadmap of the European Polysaccharide Network of Excellence to play a crucial role in the development of new generation energy storage devices by replacing synthetic polymers (Gericke et al., 2024). Current research widely explores applications, serving different functions in various devices (e.g. lignin as electrolyte oxidation preventing binder (Ma et al., 2019), as host for gel electrolytes (Xu et al., 2018), biochar precursor (Hobisch et al., 2020) or chitosan as separator (Song et al., 2024).

The use of supercapacitors, characterized by its capability to combine high power peaks and fast charging/discharging, is a key component in many modern technologies, such as consumer electronics, electric vehicles, etc. Supercapacitors consist of two electrodes, the electrolyte and a separator. The separators are typically based on synthetic polymers (e.g. PP or PE), glass fibers or cellulose. Their primary function is to provide a physical barrier between the electrodes to prevent a short circuit. However, they also enable electrolyte transport between the positive and negative electrode, where the charge storage takes place (Greenhalgh et al., 2023; Li et al., 2023; Zhong et al., 2015).

Designing a separator needs to consider technical performance as well as safety aspects at the same time (Li et al., 2023). The separator must be chemically stable to prevent unwanted reactions with electrodes or electrolytes and needs to withstand mechanical stress in wet state. The thickness of the separator also plays a decisive role. Reducing the distance between positive and negative electrodes by using a thinner separator can increase the leakage current in a supercapacitor by

---

[*] Corresponding author at: Institute of Bioproducts and Paper Technology, Graz University of Technology, Inffeldgasse 23, 8010 Graz, Austria.
E-mail address: stefan.spirk@tugraz.at (S. Spirk).

https://doi.org/10.1016/j.carbpol.2024.122354
Received 14 February 2024; Received in revised form 23 May 2024; Accepted 29 May 2024

changing the electric field between the electrodes and reducing its mechanical load barring capacity. On the other hand, thickening the separator will linearly increase the resistance (Tammela et al., 2014). Thus, an ideal separator should be between 20 and 50 μm, while maintaining the mechanical integrity in wet state (Li et al., 2023).

Besides thickness, the leakage current and ion transport resistance are affected by its permeability, pore size distribution, tortuosity, and the solvated radii of the ions. Another important design aspect of a separator is electrolyte wettability and electrolyte uptake. This impacts the infiltration time in the assembly process and also the interface impedance and thus the charging/discharging rate performance of the supercapacitor. Finally, the cost, as well as environmental aspects need to be considered. Therefore, the development of an electrochemically efficient, safe, inexpensive, and environmentally friendly separator remains a key goal for the successful charge storage application such as supercapacitors (Li et al., 2023).

Paper, as a renewable raw material with well-established and cost-efficient manufacturing processes is a good separator material already used in conventional batteries and supercapacitors. However, particularly in aqueous electrolytes, cellulose based separators (and also papers) are prone to disintegration. Nevertheless, even for aqueous based systems, the wet strength of paper separators (PS) is hardly addressed in literature (Schlemmer et al., 2021). A possible approach is to incorporate MFC (fibril bundles with diameters of 10–100 nm and lengths up to several microns) or fines to paper sheets, to achieve a denser network and to increase mechanical strength (Dufresne, 2013; Fischer et al., 2017; Hobisch et al., 2021; Siqueira et al., 2010). In order to increase wet strength further, two strategies are commercially employed. The use of wet strength agents may come with potential health risks (e.g. epichlorohydrine-polyamine complexes) (Andres et al., 2013). An environmentally friendly and safe approach would be crosslinking using carboxylic acids, which is typically employed for textile fibers and in some packaging applications in larger scale (Ma et al., 2021; Šauperl & Stana-Kleinschek, 2009; Widsten et al., 2014). Citric acid (CA) and BTCA are two commonly used polycarbonic acids for crosslinking cellulose fibers. BTCA is more effective than CA in cross-linking cellulose fibers which is owed to its tetrafunctional nature with four adjacent carboxylic functions. The presence of these functions in BTCA enhances its ability to crosslink cellulose fibers through multiple ester functions, whereas CA may result in increased surface carboxylic functions or decreased crosslinked fibers due to alternative reactions during the curing step (Awada et al., 2014; Caulfield, 1994; Zhou et al., 1995).

We hypothesize that papers with different amounts of MFCs (0–50 %) can serve as separators in aqueous based electrolytes commonly used in supercapacitors. We explored the effect of crosslinking with organic acids, particularly BTCA at elevated temperature. The influence of MFC addition as well as the influence of crosslinking was investigated and their collective impact on different separator properties, such as air permeability, thickness, density, tensile strength (dry and wet) and electrolyte uptake was studied. The performance parameters of the separators were matched with the design aspects to ensure high-performance, and above all, safe use as a separator in supercapacitors (Li et al., 2023).

2. Experimental

2.1. Materials

Zellstoff Pöls AG (Austria) supplied dried elemental chlorine free bleached softwood kraft pulp (BSKP; 85 % spruce, 10 % pine, 5 % larch) with an ISO brightness of 88 % and a Kappa Number < 5. The BSKP had a degree of polymerization (DP_V) of 3200 (determined by the intrinsic viscosity method according to ISO 5351, converted to DP_V using the Mark-Houwink-Sakurada equation (Kes & Christensen, 2013). The microfibrillated cellulose (undisclosed manufacturer) was obtained via mechanical grinding (20 passes) from bleached sulfite pulp (mixture of 80–85 % spruce and 15–20 % beech). Characterization of the raw materials (pulp and MFC) can be found in Fig. S1 to S6 and Table S1 to S3. For polyelectrolyte titration, cationic (polydiallyldimethylammonium chloride, 0.001 N, M_W 107,000 g mol^{-1}) and anionic (polyanetholsulfonic acid sodium salt, 0.001 N, M_W 9000–11,000 g mol^{-1}) standard solutions from BTG Instruments AB (Sweden) were used. All chemicals mentioned were used as received.

2.2. Pulp refining

The BSKP-sheet (30 g), was prepared according to ISO 5264-2 and subsequently beaten on a PFI-mill with 7000 revolutions. The pulp was then further suspended with tap water to reach a concentration of 2.82 g L^{-1}.

2.3. Pulp characterization

2.3.1. Carbohydrate composition

The carbohydrate composition of pulp and MFC was determined according to NREL LAP 42618 -"Determination of Structural Carbohydrates and Lignin in Biomass" (Table S1). Monosaccharides were determined by using high performance liquid chromatography (HPLC). The Agilent HPLC system uses a BioRad HPLC Carbohydrate Analysis Column Aminex HPX-87P with Guard Column Micro-Guard Carbo-P. Equipped with an Agilent Refraction Index Detector RID G1362A, using deionized water as mobile phase. Xylitol was used as an internal standard. For chromatogram evaluation the Agilent ChemStation Revision B.01.03 software (Agilent Technologies) was used.

2.3.2. Total fiber surface charge

The total surface charge of the fibers was evaluated using polyelectrolyte titration with a Charge Analyzing System (AFG Analytic GmbH, Germany). Therefore, the samples (BSKP and MFCs, 0.25 g dry weight) were first stirred for 3 h in 50 g of 0.001 N cationic PolyDADMAC titrant (107,000 $gmol^{-1}$) with 0.01 M NaCl. The solids (fibers and fines) were first removed by repeated filtration through a very fine nylon sieve and subsequently centrifuged for 15 min at 10000 rpm. Prior measurement, the supernatant phase was filtered through a syringe filter (PTFE, 0.45 μm). For charge determination 10 mL of the filtrate were titrated with 0.001 N anionic titrant (PAT, dynamically controlled rate of 0.3 mL min^{-1}) until the streaming potential reached 0 V.

Per sample three titrations were conducted to determine the total fibers surface charge q (mmol kg^{-1}), which was calculated according to Eq. 1. Where V_F is the volume of the cationic titrant consumed for the fibers and V_b the one for the blank (both in mL). The titrant concentration is given by c (mol L^{-1}) and m gives the dry mass (Bhardwaj et al., 2004).

$$q = \frac{(V_F - V_b)^*c^*1000}{m} \quad (1)$$

2.3.3. Drainability, water retention value, and fiber characteristics

The drainability was evaluated according to the Schopper-Riegler method (ISO 5267-1), while the water retention value was determined following ISO 23714 measuring three samples for the pulp and one for MFC. The morphological properties of the pulp suspension were analyzed with an L&W Fiber Tester Plus (ABB, Sweden) according to ISO 16065-2. >15,000 individual fibers per sample were measured, with each sample being repeated three times.

The morphology of the MFC was determined by atomic force microscopy (AFM) in tapping mode using a Tosca™ 400 atomic force microscope (Anton Paar, Austria) with silicon cantilevers (AP-ARROW-NCR from NanoWorld AG, Switzerland) with a constant force of 42 N $m^{-1}$and a tip radius < 10 nm. Image processing was performed with Gwyddion v2.58 software. The diluted MFC suspension with a concentration of 0.005 wt% was dried on cleaned glass slides and measured under ambient air conditions. Afterwards, the same sample was in addition coated with gold and further investigated with a Tescan Vega 3 (Czech Republic) scanning electron microscope (SEM) at an acceleration voltage of 20 kV, with the signal being detected with a secondary electron detector.

2.4. Paper separator preparation

The pulp was disintegrated (ISO 5263-1) and subsequently used, with different shares of MFC to produce hand sheets on a Rapid-Köthen sheet former (Frank PTI, Germany). The sheets, with a targeted basis weight of 18.5 g m^{-2} were formed with a pulp:MFC ratio of 100:0, 95:5, 15:85, 20:80 and 50:50 (PS-0, PS-5, PS-15, PS-20 and PS-50). Prior formation the respective amount of MFCs was disintegrated in 2 L tap water for 45 s (225 revolutions) and after the addition of the respective pulp amount for another 45 s (225 revolutions).

For the formation of the paper separators no retention aid was used. The MFC retention in the sheets was 55 to 65 % for a total MFC concentration of 5 to 50 %. Therefore, the amount of MFCs required to achieve a specific proportion was determined based on preliminary experiments. Thus, the reported values for MFC content should be regarded as estimations rather than exact measurements.

2.5. Crosslinking

The paper separators were crosslinked by means of 1,2,3,4-butanetetracarboxylic acid (BTCA, Sigma Aldrich; 7 wt% in distilled water). To catalyze the process, 50 % sodium hypophosphite monohydrate (Sigma Aldrich), based on the weight of BTCA, was added. Filter papers (Rotilabo, type 113 A, ⌀ 185 mm) were soaked with 5.2 g of BTCA solution, placed on the hand sheets to fully impregnate them, and then dried at 93 °C for 10 min under vacuum (100 mbar). To initiate the crosslinking, the impregnated sheets were then treated at 170 °C for 140 s. For the washing step, the crosslinked sheets were placed on a 300-mesh sieve and 2.0 L of distilled water were filtered through using a vacuum pump. In addition, one batch solely impregnated with water instead of BTCA has been produced as blank and herein named with the suffix “BLANK”.

The BTCA- treated papers are named with the suffix “BTCA” (PS-0-BTCA, PS-5-BTCA, PS-15-BTCA, PS-20-BTCA and PS-50-BTCA) and in the corresponding figures, colored by an orange toned colour. In contrast, the untreated samples are named with the suffix “NEAT” (PS-0-NEAT, PS-5-NEAT, PS-15-NEAT, PS-20-NEAT and PS-50-NEAT) and are visually represented in green tones. The weight of the papers was between 0.58 and 0.60 g.

2.6. Paper separator characterization

Before conducting the experiments, all paper separators were conditioned for 24 h (at 23 °C, 50 % relative humidity) following ISO 187. The thickness and the apparent sheet density were subsequently assessed in accordance with ISO 534, with minimum 20 measurement points. The thickness for z-directional expansion was determined according to ISO 12625-3, with a pressure of 2 kPa.

Air permeability was measured according to the Gurley method, following the procedures outlined in ISO 5636-3, with a minimum of 12 measurement points. The tensile (dry) strength was evaluated according to ISO 1924-2, utilizing a tensile tester (FRANK-PTI, Germany), with at least 12 measurements were taken. The wet strength determination was following the same procedure as dry tests, with soaking the sample for 15 s in distilled water, as suggested in ISO 12625-5. Soaking tests have been performed by immersing the 15 mm broad paper strips for 7 days (at 23 °C) in 1 M $NaNO_3$. Prior tensile testing according to ISO 1924-2, the 10 strips were thoroughly rinsed with deionized water. To record stress, strain curves and calculate thereof the modulus of elasticity, 5 samples per separator were tested on a Zwick Roell (Germany) Z010 tensile tester with a clamping length of 50 mm and a testing speed of 5 mm min^{-1}. Light micrographs were taken with a Axio Scope.A1 (Zeiss, Germany). The surface morphology of the paper separators was investigated with a SEM Vega 3 (Tescan, Czech Republic) at 3 kV, detecting the signal with a secondary electron detector from the gold coated samples.

2.7. Fourier-transform infrared spectroscopy

To distinguish in the overlapping band between the ester and carboxylic function, the samples were placed for 5 min in a 0.1 M NaOH aqueous solution at room temperature, to convert the carboxyl groups into carboxylate, which shows an absorbance band at 1590 cm^{-1} (Awada et al., 2014). Afterwards, the samples were dried at 40 °C for 24 h and subsequently investigated with an ALPHA FT-IR (Bruker) with an attenuated total reflectance module. The samples were scanned 32 times with a resolution of 4 cm^{-1}. The spectra were baseline corrected and normalized to the band at 1313 cm^{-1} (cellulose C—H band) and the data were further processed and analyzed with Origin data analysis software (OriginLab Corporation) (Yang et al., 1996).

2.8. Electrolyte uptake

Electrolyte uptake (EU) tests were performed under standard environment (23 °C, 50 % relative humidity) according to ISO 535, Annex B, with slightly adopted testing conditions: the 3 × 3 cm^2 samples were weight (w_0) and immersed for 60 min (w_{60}) in 1 M aqueous $NaNO_3$. Before determining the wet weight, the samples were hold vertically on a corner for 30 s. The remaining drop at the bottom corner was removed with a blotting paper. In total the procedure was repeated at least 12 times and the EU (%) was determined according to Eq. (2).

$$\mathrm{EU} = \frac{(w_{60} - w_0)*100}{w_0} \tag{2}$$

2.9. Heat resistance

For heat resistance (HR) tests, the samples got shafted into 2 × 2 cm^2 squares and placed for 5 min in an oven (Binder, Germany) at 105, 150 and 200 °C.

The shrinkage was calculated based on Eq. (3), while A_0 is the surface area before, and A_5, after the heat treatment.

$$\mathrm{HR} = \frac{A_5*100}{A_0} \tag{3}$$

2.10. Contact angle measurements

The contact angle was determined on a Dataphysics OCA200 by applying 1 μL drop of 1 M $NaNO_3$ (at 23 °C; 50 % relative humidity) onto the 1 cm broad paper separator strips. The behavior of the drop was recorded by a high-speed camera and evaluated using the Dataphysics software.

2.11. Electrochemical characterization

Electrochemical impedance spectroscopy measurements were carried out by a BioLogic VMP-300 Potentiostat (Paris, France) within the frequency range of 1 MHz to 1 mHz at open circuit potential (~30 mV). Carbon/carbon symmetric Swagelok type supercapacitor cells were constructed using 1 M aqueous $NaNO_3$ electrolyte. The activated carbon used was commercial YP80 F (Kuraray, Japan). Electrodes were produced from a mixture of 90 wt% of YP80 F, 5 wt% of carbon black SUPER C65 (Imerys, France) as a conductivity enhancer, and 5 wt% of polytetrafluoroethylene (PTFE, 60 wt% suspensions in water, Sigma-Aldrich, USA) as a binder. These three components were mixed in isopropanol and the mixture was stirred at 70 °C until a homogeneous dough was obtained, which was rolled onto a glass plate to produce a sheet. The carbon sheet was dried at 80 °C overnight and the sheet with final thickness of ~100 μm was obtained. Electrodes in circle-shape with a diameter of 10 mm and similar mass (Table S9) were punched out to construct supercapacitor cells. The electrodes were sandwiched between stainless steel current collectors and separated by herein produced paper separators (⌀ = 12 mm; PS-0-BTCA, PS-5-BTCA, PS-15-BTCA, PS-20-BTCA and PS-50-BTCA), commercially available GF/A (Whatman Filter, UK) or PP (polypropylene-based separator from Nippon Kodoshi Corporation, Japan), which were soaked with electrolyte. From the distinguished regions of the cell Nyquist plots, various resistances such as equivalent series resistance, charge transfer resistance, ion diffusion resistance and equivalent distribution resistances were extracted. Finally, charging/discharging rate performance values for each cell were calculated by utilizing the knee-frequency values at maximum imaginary capacitance. Galvanostatic cycling with potential limitation (GCPL) was carried out within a window of 0 V to 1.2 V applying a current load of 0.5 A g^{-1} to reveal the performance of separators towards 7500 cycles of use. The effect of charge/discharge cycling has been expressed in terms of capacitance retention %, Ohmic drop, Coulombic efficiency % and energy efficiency % adopting the method described by Laheäär and coworkers (Laheäär et al., 2015). Finally, cyclic voltammograms (CV) were recorded within several potential windows at a scan rate of 2 mV s^{-1} to ascribe the long term cycling performance.

3. Results and discussion

3.1. Paper separator characterization

The incorporation of MFCs (up to 50 wt%) into paper separators utilized for energy storage applications serves three primary objectives, namely to generate a denser fiber network to (i) reduce porosity, (ii) to enhance the strength and (iii) to mimimize their thickness.

MFC addition allows to adjust permeability and thickness.

Transmission light microscopy and SEM images (Fig. 1d-h and Fig. 2, respectively) confirm a homogeneous distribution of MFCs throughout the paper separator. Light micrographs reveal a transition from a porous network with proportionally more thicker fibers (PS-0) towards a denser network (PS-50) upon MFC addition. This results in an all-cellulose composite where pulp fibers form a scaffold, which is reinforced by the fibrillar MFC network (Hobisch et al., 2021). With the subsequent addition of MFCs, the proportion of thick pulp fibers is reduced, thus making the paper separator thinner (Fig. 1a). Because of the thickness decrease, the apparent density increases (Fig. 1b) as grammage remained rather constant throughout all prepared sheets (18.3–18.9 g m^{-2}, Table S4). In the absence of MFCs, the paper separators exhibit irregularly distributed pores ranging from 10 to 60 μm. Those voids can be reduced to 1–30 μm (5 % MFC) and even further with successive addition of MFCs (Fig. 1d-h). The denser fibrillar network and subsequent pore-filling decreases the air permeability, suggesting also a reduced ion permeation (Fig. 1c). At PS-50, a network of such density is attained that air can barely permeate (<0.1 cm^3 s^{-1}). The reduction in permeability with the subsequent addition of MFCs is consistent with literature as it is (roughly) proportional to the fourth power of the fiber thickness (Shallhorn & Gurnagul, 2009). Microtome cuts (Fig. S7) further illustrate the reduction in thickness, depicting a decrease in bulky pulp fibers with an increased share of fine, fibrillated MFCs. The distribution of MFCs across the cross-section of the separators appears uniform.

While maintaining a certain level of permeability is desirable for separators to facilitate rapid ion transport, a denser network can increase the resistance of supercapacitors. During the operation of a supercapacitor it may occur that carbon particles detach from the electrode surface. If the void diameter exceeds the carbon particles of the electrode, a short circuit may be induced (Li et al., 2023). Therefore, designing a separator for supercapacitors (or batteries), it is important to bear in mind its main role: serving as an ion-permeable physical barrier to prevent short circuits between the positive and negative electrodes (Greenhalgh et al., 2023).

BTCA treatment notably effects surface morphology and density.

The BTCA-treated samples exhibit a distinctly smoother surface compared to the untreated ones. There is a transition from fibrils being exposed on the surface (NEAT) towards a smoother surface after BTCA treatment, where fibrils have been mostly interconnected and covered. Process induced effects can be ruled out, as shown in Fig. S8 for blank samples. The BTCA treatment results in a less fibrillated network, thereby potentially enhancing the papers permeability (Fig. 1c).

Additionally, the slightly noticable raise in the averaged air permeability after crosslinking can be attributed to the decreased availability of hydroxyl groups. This reduction enables the fiber network to uphold its dimensional integrity within the specified testing conditions (23 °C; 50 % relative humidity) as it is less prone to swell (Häggkvist et al., 1998; Korpela et al., 2023; Lund & Brelid, 2014; Šauperl & Stana-

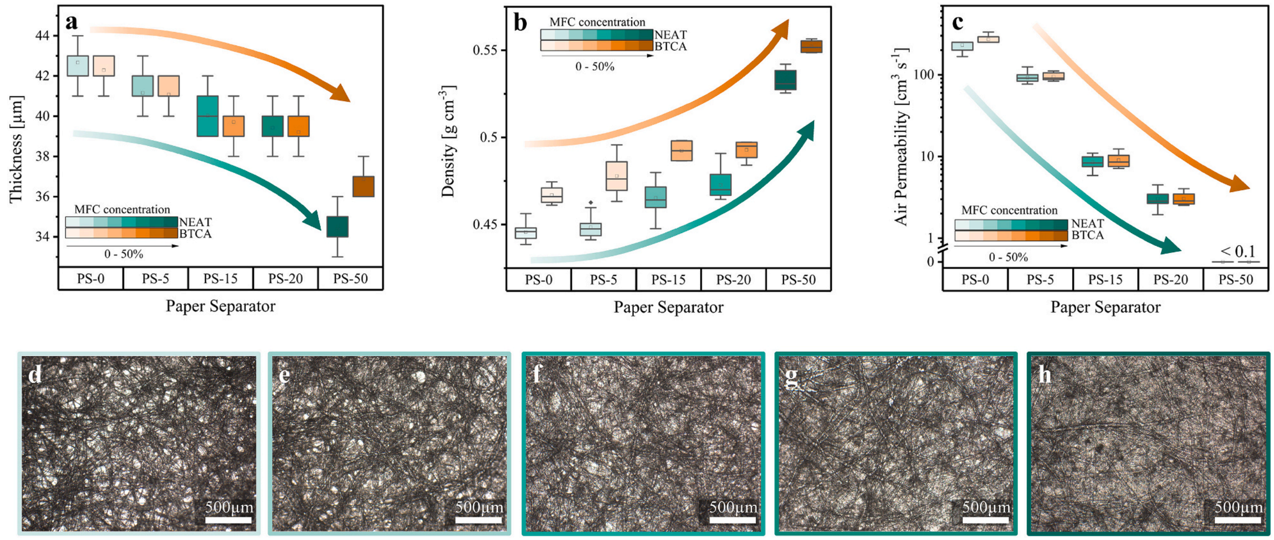

Fig. 1. The graphs show a decreasing thickness (a), increasing apparent density (b) and a decreasing air permeability as the MFC content increases, for the NEAT and BTCA treated samples. Light microscopy images of the NEAT papers highlight a denser network (d-h) with an increasing MFC content.

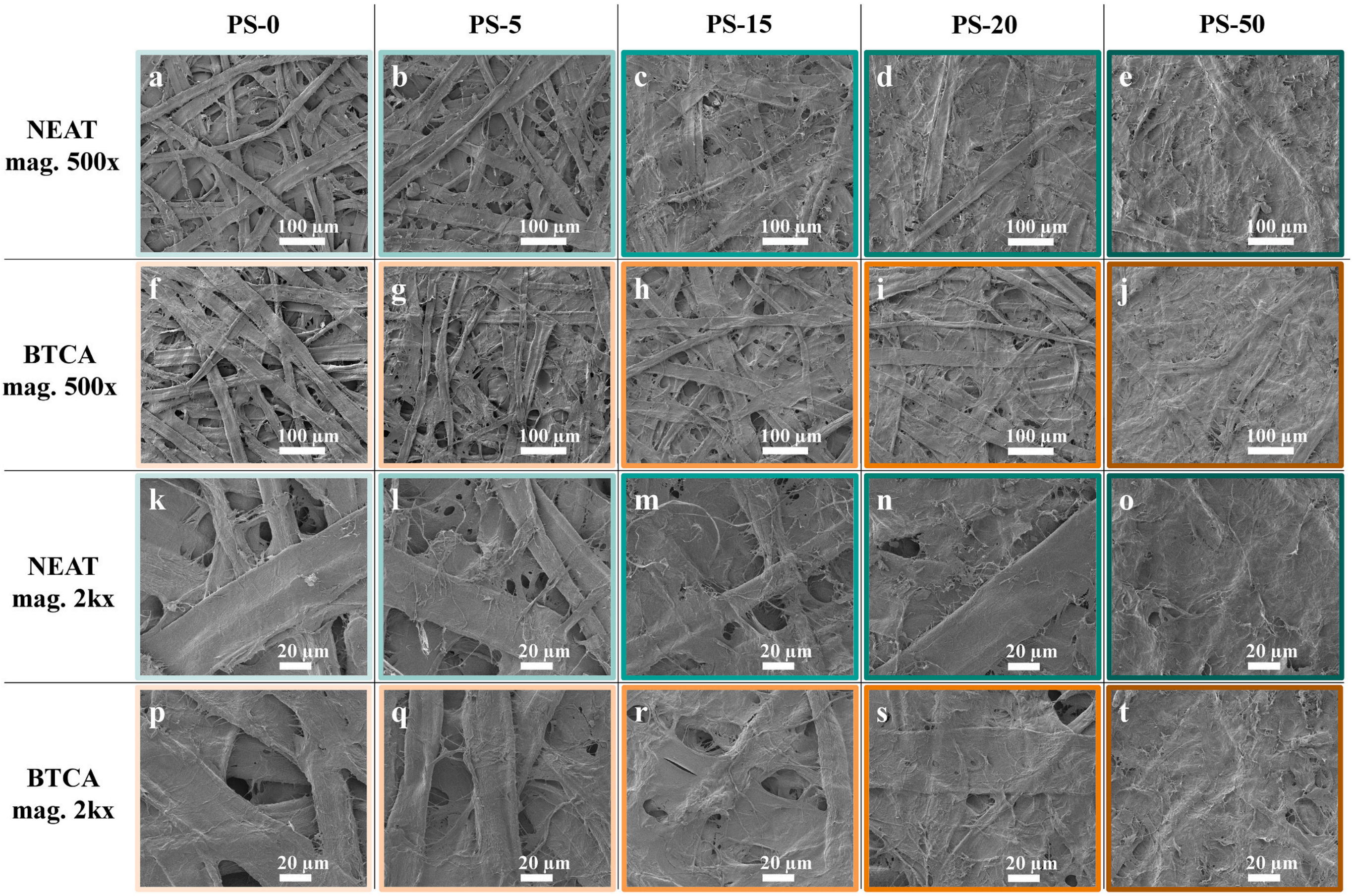

Fig. 2. SEM images at a magnification of 500× of NEAT (a-e) and BTCA treated (f-j) and 2kx of NEAT(k-o) and BTCA (p-t) treated paper separators from PS-0 to PS-50, respectively. An increasing MFC content reveals a denser network, while BTCA treatment reveals a smoother surface morphology.

Kleinschek, 2009; Shallhorn & Gurnagul, 2009).

Consequently, also the swelling capacity of the BTCA treated papers decrease compared to the other samples as water is not able to penetrate as efficiently in between the fibril and fiber surfaces. This is further supported by swelling tests in the z-direction (Table S5). The findings show that paper separators treated with BTCA are more likely to maintain their thickness and are dimensionally stable in z-direction. While the thickness of neat paper separators increased by approximately 50 %, the BTCA-treated ones exhibited only an 8 % increase (mean value). This is an important point in supercapacitor design as electrolyte-induced swelling may increase significantly the electrode contact pressure. A controlled, minor swelling may be beneficial for energy storage assembly (e.g., pouch cells or cylindrical cells), facilitating enhanced cohesion among cell components. This leads to a better contact between electrodes and the separator, thereby reducing contact resistance and subsequently improving the power performance (Ahankari et al., 2022; Toigo et al., 2020).

The increase in density (Fig. 1b) after the crosslinking treatment suggests a BTCA-induced modification in the paper. However, it is important to note that changes induced by density do not a priori reflect the formation of ester bonds but may also be explained by physical interactions of the acid in the sheet. It should be noted here that the equilibrium moisture content (at 23 °C; 50 % relative humidity) is between 6 and 6.5 % (for both PS-NEAT and PS-BTCA Table S6). In order to reveal the crosslinking success, IR spectroscopy is required.

3.2. *BTCA successfully formed ester bonds*

The interaction between cellulose and BTCA (as well as other carboxylic acids) takes place in a two-stage esterification process at elevated temperatures. Initially, two adjacent carboxyl groups within the BTCA undergo dehydration, which leads to the formation of a five-membered cyclic anhydride intermediate, catalyzed by an alkaline salt (e.g., sodium hypophosphite). Subsequently, the anhydride reacts with the cellulose hydroxyl groups forming covalent ester bonds (Awada et al., 2014; Ji et al., 2015; Kokol & Vivod, 2023). As a side product, grafted cellulose can form, which carries only one ester bond (Kono & Fujita, 2012). The formation of the grafted product can be disfavored by low BTCA:cellulose ratios as we use in this paper (ca. 1:10).

A successful cross-linking of the BTCA treated paper is evident by analysis of the FTIR spectra (Fig. 3). The neat samples (Fig. 3a and S9, non-crosslinked, alkali treated) do not exhibit any bands related to esters, but an increasing band related to adsorbed water (1648 cm^{-1}), which increases with increasing MFC concentration in the separators. After crosslinking of the papers with BTCA followed by mild alkaline treatment (0.1 M NaOH) new bands appear at ca. 1730 and 1580 cm^{-1} which become more intense at increasing MFC concentration (Fig. 3b, Fig. S10). This can be explained by the higher surface area of MFC compared to the pulp fibers, offering more potential sites for cross-linking with BTCA. The bands at 1730 cm^{-1} represent $\nu_{C=O}$ bands assigned to ester bonds between BTCA and the cellulose fibers while the one at 1580 cm^{-1} can be assigned to ν_{COO^-} in the non-crosslinked parts of the BTCA. The successful ester bond formation is also visible in the δ_{OCO} at 1250 cm^{-1} which is increasing in intensity at higher MFC concentrations. Similar observations of BTCA crosslinking have been made by other authors (Awada et al., 2014; Ma et al., 2021).

It should be noted here, that the degree of crosslinking using BTCA for cellulosic materials can be in principle also determined using ^{13}C

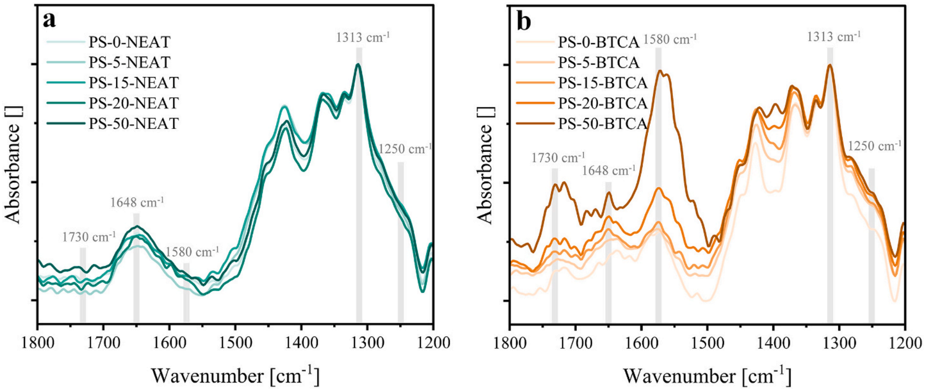

Fig. 3. ATR-FTIR-spectra after mild alkali treatment with 0.1 M NaOH of NEAT (a) and (b) BTCA treated paper separators showing a successful crosslinking with BTCA at the C=O band (~1730 cm^{-1}).

solid-state NMR spectroscopy, allowing for a quantification of the crosslinking reaction. This is a particularly convenient approach for highly swollen materials or hydrogels (Kono & Fujita, 2012), where a homogenous crosslinking of all cellulose molecules by BTCA is favored. For our separators, this approach is less straightforward as we employ fibers whose surfaces are crosslinked, i.e., in the solid-state NMR spectra we would observe rather large bulk signals which are difficult to resolve from crosslinked molecules.

3.3. BTCA treatment increases the wet strength by over 6000 %

High mechanical strength and stability of a separator are important to ensure the safety of the supercapacitor. As a reference, 0.3 kN m^{-1} has been suggested to withstand the mechanical forces encountered during assembly and operation (Greenhalgh et al., 2023; Li et al., 2023; Zhong et al., 2015). The mechanical properties were determined under both dry and wet conditions (Fig. 4a and b, respectively). For the neat paper separators, the tensile strength in dry state (Fig. 4a) increased from around 1 kN m^{-1} (PS-0-NEAT) up to a maximum of around 1.3 kN m^{-1} (PS-20-NEAT). The wet strength (Fig. 4b) showed a nearly twofold increase (compared to PS-0-NEAT) with rising MFC concentration, peaking at 50 % (PS-50-NEAT). A similar trend was reported for bagasse pulp where a threefold increase in wet strength was observed with up to 40 % MFC addition, after which a plateau was reached (Hassan et al., 2011).

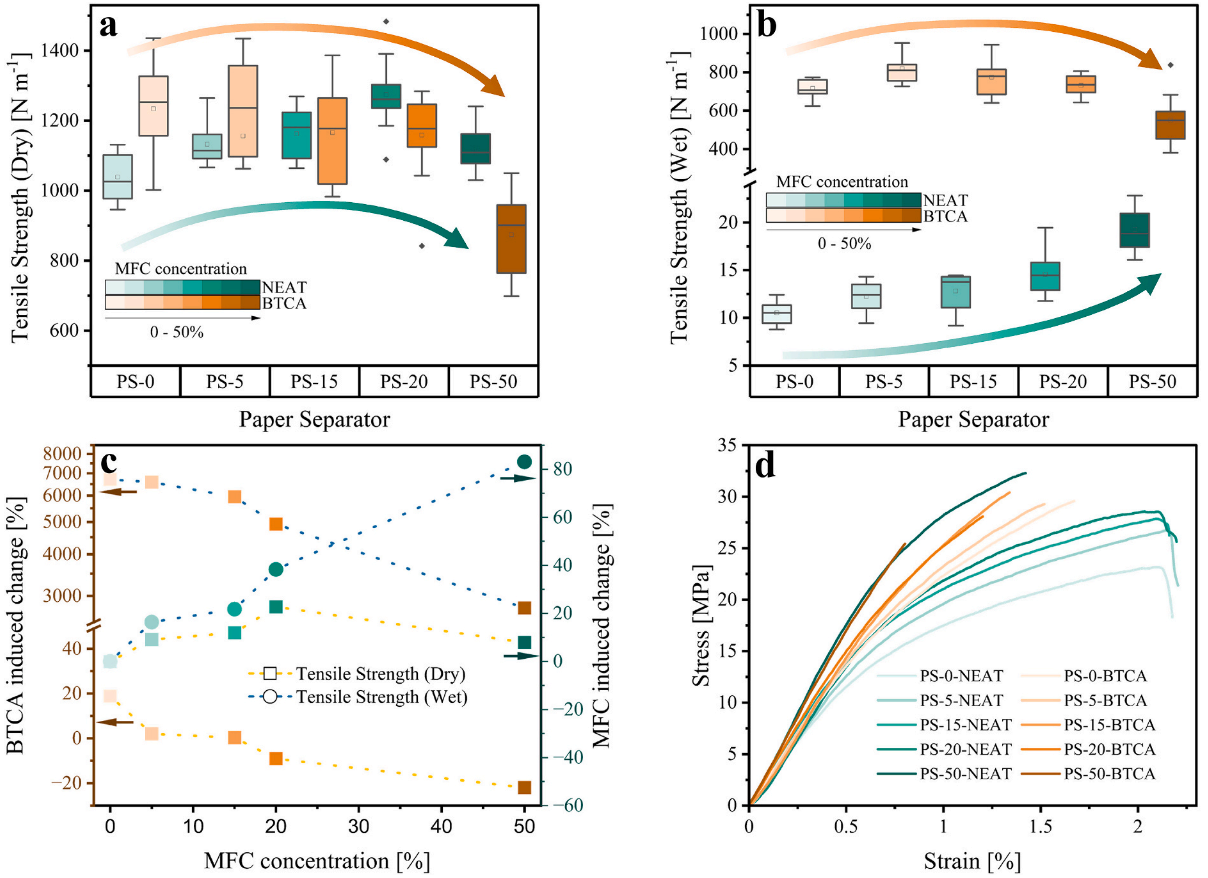

Fig. 4. Dry (a) and wet (b) tensile strength of neat and BTCA treated paper separators (c) showing the MFC and BTCA induced changes in mechanical properties and (d) representative stress-strain curves.

Despite the notable increase in wet strength observed when comparing PS-0-NEAT to PS-50-NEAT, the measured value of 19 N m^{-1} remains considerably lower than the target value of 300 N m^{-1}, especially under conditions of full moisture saturation (Li et al., 2023).

The modulus of elasticity increases with a rising share of MFCs (Table S7). In Fig. 4c, stress-strain curves for PS after BTCA treatment illustrate that the slope of the curve increases but the plastic region and the strain-at-break clearly decreases. At PS-50-BTCA, this region is non-existent and elongation only takes place in a short, elastic range until brittle break. The effect of crosslinking derived embrittlement has been well noted in literature. It can be explained by the lower relative flexibility of the cellulose chains. This in turn reduces the formability of the fibers (and in consequence its network) in this herein generated all-cellulose composite (Caulfield, 1994; Korpela et al., 2023; Quellmalz & Mihranyan, 2015).

Crosslinking the paper separators with BTCA could enhance the dry strength until a maximum of 20 % to about 1.25 kN m^{-1} for PS-0-BTCA, whereas no noticeable increase was observed for PS-5-BTCA and PS-15-BTCA (Fig. 4 b,c). Conversely, paper separators with 20 % and 50 % MFCs exhibited a negative impact from crosslinking, resulting in decreases of −10 % and 20 %, respectively (Fig. 4c). The effect of the BTCA treatment on the wet strength of the paper separators was, however, tremendous. The maximum increase, reaching astonishing 6700 % for PS-0-BTCA, is to the best of our knowledge, the highest ever reported thus far. Although the absolute wet strength values decrease, with an increasing share of MFCs, the overall impact of the BTCA treatment remains impressive with an increase of still close to 3000 % for PS-50-BTCA (Fig. 4c). The paper separators show a similar trend with slightly decreased strength after being soaked for 7 days in 1 M $NaNO_3$ (Fig. S11). However, the values remain within the standard deviation and above 300 N m^{-1}.

3.4. Paper separators are thermally stable up to 200 °C

The thermal stability is a crucial factor for a successful separator design. Charging and discharging a supercapacitor at high current rates can result in heat generation, potentially leading to thermal runaway reactions in worst case (Kumaravel et al., 2020). Special attention must be paid to the use in areas where high temperatures are reached, such as military, aviation, oil drilling or space research (Kumaravel et al., 2020). Thus, all components, including the separator, must maintain their structural integrity under high temperatures. In combination with the appropriate electrolytes, such as ionic liquids which are inflammable and have a low vapor pressure, this can further enhance safety and performance (Zaccagnini et al., 2023).

Heat resistant tests showed that there was no thermal induced shrinkage in PS-NEAT, nor in PS-BTCA up to 200 °C. However, a slight yellowing was observed with increasing temperature for PS-BTCA (Fig. S11). This effect is most likely to occur from an aconic acid oligomer at elevated temperatures (Ke et al., 2020; Ye et al., 2015).

The commercially available separator GF/A did not show thermal induced size reduction (HR = 100 %), while the PP area left after heat treatment (at 200 °C) was only 13 % compared to its original shape. This is well reported among literature and recognized as a common safety concern with synthetic polymer separators (Zhang et al., 2018).

3.5. Electrolyte uptake is highly influenced by BTCA treatment, but less by MFC content

An important design aspect is the dimensional stability (Li et al., 2023). Especially during assembling of supercapacitor cells, the neat paper separators show a clear disadvantage when being wetted. While BTCA separators retain their 2-dimensional structure, PS-NEAT tend to curl up and fold, especially when additional forces (such as gravity) are present (see Fig. 5 a vs. b). This makes the assembly process tedious to impossible.

Another important separator design parameter is the electrolyte wettability of the separator to reduce the wetting time and the ion transport resistance and to increase the power density of the supercapacitor (Szubzda et al., 2014). In this case, electrolyte uptake and contact angle measurements are a good indicator. The average electrolyte uptake of the neat papers varies between 365 % and 381 % and is hardly increased by incorporation of MFCs (Fig. 5c). However, the effect of BTCA crosslinking reduces the electrolyte uptake by approximately 50 %. Fig. 5d-h demonstrate an increasing contact angle with increasing MFC content.

In general, the water uptake capability of paper is significantly affected by hornification. Hornification is commonly referred as a process where water from cellulosic materials are removed at elevated temperatures. This process is irreversible and characterized by an aggregation of microfibrils, leading to lower water (vapor) uptake capabilities and higher hydrophobicity as shown for celluose model materials (Ehmann et al., 2015; Reishofer et al., 2022). In this context, BTCA-treated papers undergo two additional wetting and heating steps, which could amplify the effect of hornification. Further, it has been reported, that a short interruption in the drying process up to 140 °C,

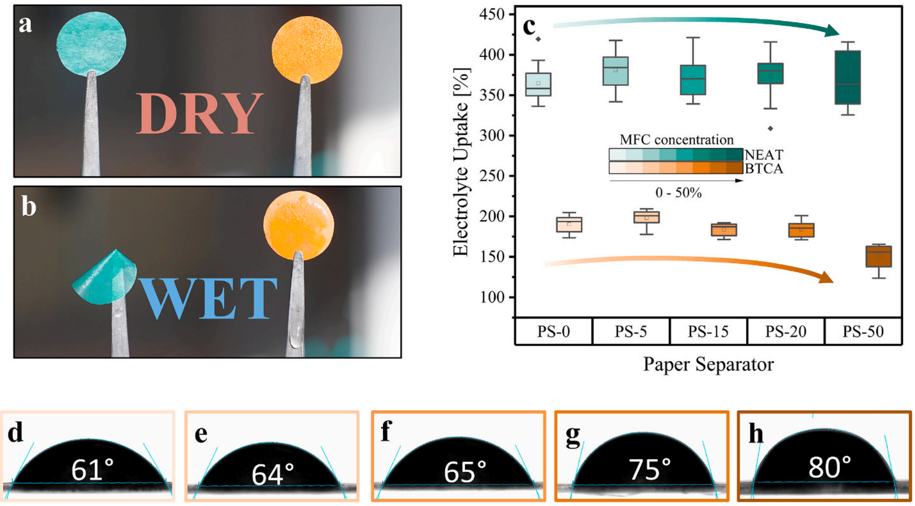

Fig. 5. Colored PS-15 (green: NEAT, orange: BTCA, ⌀ = 15 mm) separators demonstrating their dimensional stability before (a) and after being wettened (b); Electrolyte Uptake of neat and BTCA samples (c) and images of the contact angle of 1 M $NaNO_3$ when being received (d-h) for PS-BTCA-0 to PS-BTCA-50, respectively.

when the paper is not fully dry yet, leads to a higher content of hornified fibers (Salmén & Stevanic, 2018). This also happens during the crosslinking procedure: The papers are pre-dried to approximately 5–15 % until the drying process gets interrupted and the paper separator is further placed for 140 s at 170 °C. If even higher water affinity is desired, the BTCA crosslinked papers can be treated with NaOH. Thereby, the carboxyl groups are deprotonated, which increases the water affinity and thus the absorption capacity towards aqueous media (Kono & Fujita, 2012).

3.6. *Electrochemical characterization*

3.6.1. *Performance approaches the commercial references*

Nyquist plots obtained for the carbon/carbon symmetric supercapacitor cells with the employed paper separator PS-0-BTCA to PS-50-BTCA are presented in Fig. 6a, b. For comparison, commercially available samples GF/A and PP were used and the impedance data of the herein assembled supercapacitors were compared. The resistance values extracted from the impedance data are presented in Table 1.

A progressive increase of equivalent series resistance is due to the electrolyte resistance that indicates the electrolyte transport from the bulk to the electrode porosity. As the share of MFCs increases, the bulk electrolyte transport to the electrode is influenced, reaching the highest value of 3.2 Ω for PS-50-BTCA. In contrast, values of 0.47 and 0.51 for GF/A and PP respectively indicate low resistance for the electrolyte transport from bulk to porosity. The charge transfer resistance also increases gradually with an increasing share of MFCs which could be due to their involvement in increased resistance of electrode/electrolyte interface.

Since the current collector and mass of the carbon electrode (Table S9) used in this work is the same across all the cells, it can be inferred that the charge transfer resistance originated from the total resistance of electrode/electrolyte under bulk conditions.

The diffusion of ions is also influenced by the type of separator used in the supercapacitors. The low values of 0.87 Ω and 1.1 Ω for GF/A and PP, respectively, are in a comparable range to PS-0-BTCA to PS-20-BTCA. However, the ion diffusion is impacted at a 50 % MFC content (PS-50-BTCA). These influences can be also seen in equivalent distribution resistance values which indicate cumulative resistance across the bulk electrolyte to bulk electrode. The overall resistance levels from PS-0-BTCA to PS-20-BTCA fall within a similar range to those of the commercial separator samples. The PS-50-BTCA separators show a different behavior though. Overall, it can be concluded that the presence of high amounts of MFC in the separator negatively impacted the performance of supercapacitors which directly influences the power output and rate at which supercapacitors can be charged and discharged. In particular, the time constant of sample PS-15-BTCA and PS-20-BTCA is in comparable range of GF/A and PP. From the Nyquist plot data, sample PS-20-BTCA appears closer to the commercial samples.

Table 1
Charge/discharge time constant (τ) equivalent series resistance (ESR), charge transfer resistance (CTR), ion diffusion resistance (IDR) and equivalent distribution resistance (EDR) of PS-BTCA, GF/A and PP separators.

	τ [s]	ESR [Ω]	CTR [Ω]	IDR [Ω]	EDR [Ω]
PS-0-BTCA	*	0.83	1.21	1.07	2.37
PS-5-BTCA	*	0.85	1.26	1.09	2.55
PS-15-BTCA	1.21	1.52	2.17	0.78	3.99
PS-20-BTCA	1.19	1.89	3.04	1.04	5.78
PS-50-BTCA	15.6	3.25	49.57	15.80	66.18
GFA	0.33	0.47	0.24	0.87	1.39
PP	0.38	0.51	0.27	1.10	1.34

* not applicable due to the undefined maximum imaginary capacitance (Fig. S13).

To assess the long-term stability, GCPL curves were recorded over 7500 consecutive cycles (Fig. 7) and evaluated in terms of capacitance retention %, Ohmic drop (Fig. 7c and d, respectively), Coulombic efficiency, and energy efficiency (Fig. S14). As expected, the observed impedance trends across different MFC concentrations in the separator correlate with the variations in Ohmic loss and other performance metrics.

PS-15-BTCA and PS-20-BTCA (details in Fig. 7a and b, respectively) demonstrate a comparable range of Ohmic drop values to GF/A and PP (details in Fig. S15), remaining relatively stable over 7500 cycles, resulting in negligible decay in capacitance retention %. In contrast, PS-5-BTCA and PS-50-BTCA exhibit higher initial Ohmic drop values, with PS-5-BTCA showing an increase in Ohmic drop and a decrease in capacitance retention % over extended cycling, while PS-50-BTCA shows the opposite trend. Similar trends of Ohmic drop for different MFC content are evident in their corresponding cyclic voltammogram as well (Fig. S16).

The lower MFC content in PS-5-BTCA leads to a less dense network

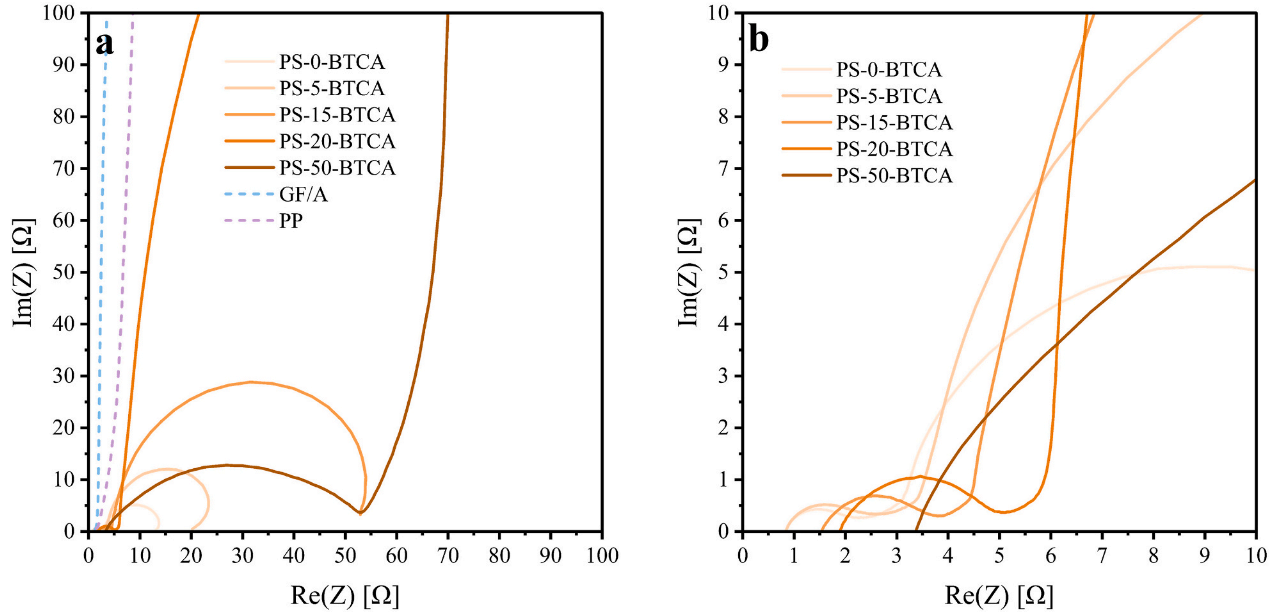

Fig. 6. Nyquist plots for PS-BTCA, PP and GFA (a) and PS-BTCA in more detail (b).

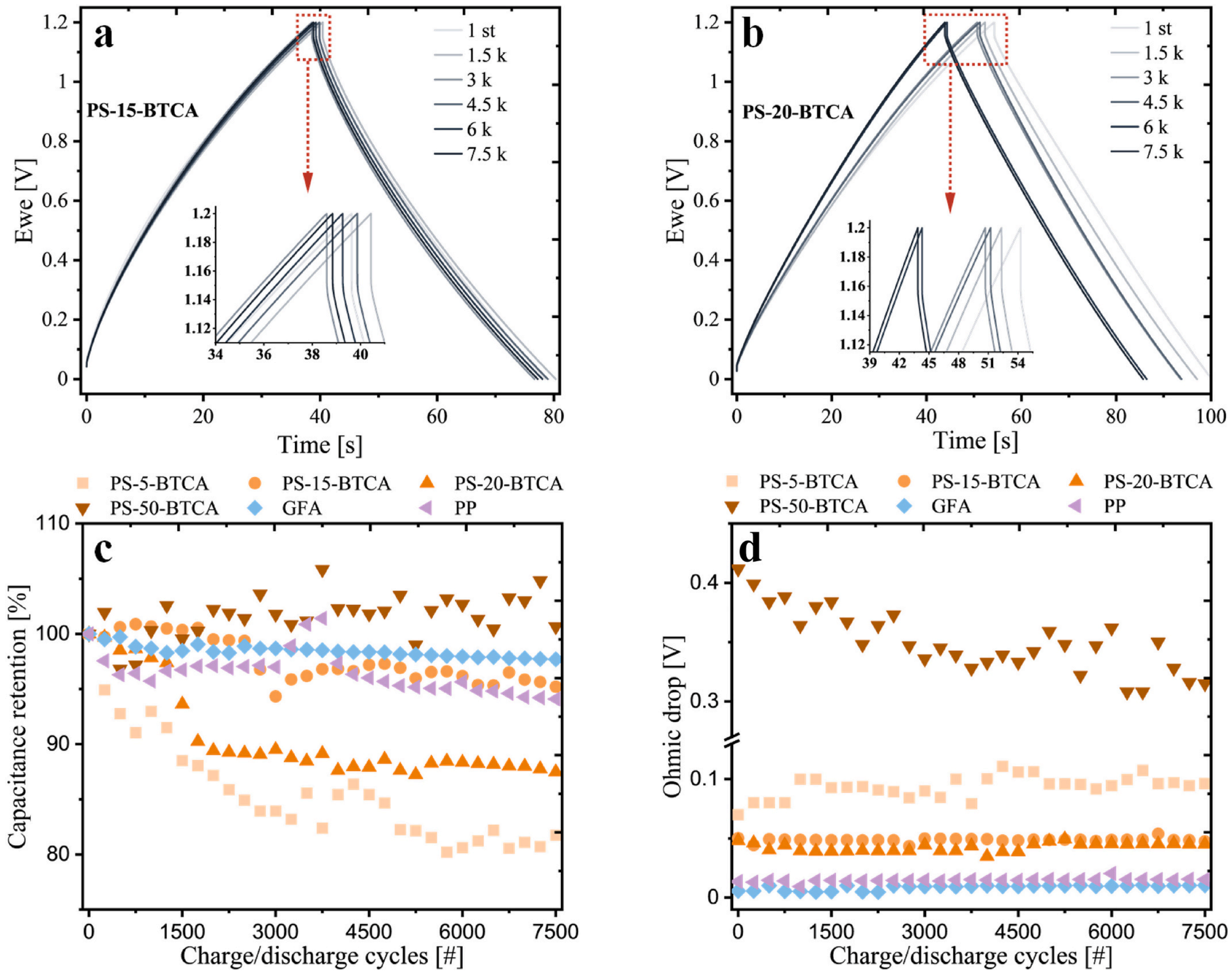

Fig. 7. Effect of charge/discharge cycles numbers (potential window: 0 V to 1.2 V and current loading: 0.5 A g^{-1}) on the GCPL of better performing separators (a) PS-15-BTCA, (b) PS-15-BTCA, (c) capacitance retention %, and (d) Ohmic drop, Coulombic efficiency and energy efficiency for different separators.

with larger pores that initially facilitate ion transport but may also lead to an increased Ohmic loss due to longer ion pathways. With prolonged charge/discharge cycles, the physical integrity of the separator may deteriorate, resulting in pore collapse, increased tortuosity, and other microstructural changes, contributing to higher Ohmic drop and reduced capacitance retention %.

The moderate MFC content in PS-15-BTCA and PS-20-BTCA likely attains a balance between sufficient microfiber density for structural integrity and porosity for ion transport. This composition minimizes the Ohmic drop by maintaining adequate ion pathways while ensuring microstructural stability similar to commercial GF/A or PP separators. The MFC content of 50 % in PS-50-BTCA results in a dense and compact separator structure, initially slowing ion transport (Table 1) and increasing the Ohmic drop. However, over thousands of cycles, PS-50-BTCA may undergo physical reorganization due to cycling-induced microstructural deformation, potentially leading to improved ion transport efficiency and reduced Ohmic drop, ensuring higher capacitance retention %. As such, the dominance of MFC content in the separator also impacts the rate of charge storage and release, as evidenced by Coulombic efficiency and energy efficiency, which follow a similar pattern as observed in other electrochemical performances.

4. Conclusion

In this work, we investigated the influence of MFC and a crosslinking treatment via BTCA on paper separators for energy storage applications, in particular supercapacitors. Therefore, paper separators were produced via a simple paper making approach and their properties characterized bearing necessary design aspects in mind, to ensure a safe operation and a high charge performance.

Through the integration of MFCs into the paper matrix, we were able to fabricate paper separators with a thickness below 40 µm. The successive addition of MFCs also led to a densification of the network, resulting in a progressive reduction in permeability. However, a denser network also aids to mitigate the formation of conductive physical bridges between the two electrodes, which in turn could potentially lead to a short circuit.

Although the wet strength could be improved by 80 % with subsequent addition of MFCs to a maximum of 19 N m^{-1}, it remains far below the necessary requirements (>300 N m^{-1}). However, employing BTCA induced crosslinks, we were able to enhance the wet strength by more than remarkable 6000 % to approximately 800 N m^{-1} (for 5 and 15 % MFC addition) while maintaining the dry strength at about 1150 N m^{-1} (for 5 to 20 % MFC addition). Further, crosslinking ensures the separators dimensional stability under wet conditions, thereby preventing curling during handling which guarantees an easy assembling of the storage device. However, crosslinking also comes with some downsides, such as embrittlement, reduced electrolyte uptake and increased absorption times.

Electrochemical impedance spectroscopy measurements showed that with a subsequent increase of MFCs, the resistance values increased, with a charge/discharge time constant comparable to commercial separators for a share of 20 % MFCs. Galvanostatic cycling with potential limitation showed, that separators with 15 % and 20 % MFCs retain their considerably low Ohmic drop on a constant level over 7500 cycles.

Overall, our work demonstrates that the network of this cellulose-based composite could be easily tailored by the addition of MFCs, and also that crosslinking cellulose separators is of high importance to ensure a reliable assembly and safe operation.

Funding

This work was partially funded by the Academy of Finland's Flagship Programme under Project Nos. 318890 and 318891 (Competence Center for Materials Bioeconomy, FinnCERES). This research has also received funding from the European Innovation Council (EIC) under grant agreement No 101115293 (VanillaFlow).

CRediT author statement

Statement: During the preparation of this work the author(s) used DeepL Translator and GPT-3.5 to find appropriate synonyms, phrases and linking text blocks to better explain the subject and make the text more coherent. After using this tool/service, the author(s) reviewed and edited the content as needed and take(s) full responsibility for the content of the publication.

Julian Selinger: Conceptualization, Methodology, Investigation, Validation, Formal analysis, Writing – Original Draft.

M. Tauhidul Islam: Conceptualization, Methodology, Investigation, Validation, Formal analysis, Writing – Review & Editing.

Qamar Abbas: Conceptualization, Methodology, Writing – Original Draft, Review & Editing.

Jana B. Schaubeder: Investigation, Methodology, Formal analysis, Writing – Review & Editing.

Janis Zoder: Investigation, Formal analysis, Writing – Review & Editing.

Adelheid Bakhshi: Methodology, Investigation, Writing – Review & Editing.

Wolfgang Bauer: Conceptualization, Methodology, Writing – Review & Editing.

Michael Hummel: Conceptualization, Writing – Review & Editing.

Stefan Spirk: Conceptualization, Methodology, Supervision, Writing – Review & Editing.

Declaration of competing interest

The authors declare that they have no known competing financial interests or personal relationships that could have appeared to influence the work reported in this paper.

Data availability

Data will be made available on request.

Acknowledgement

The authors would like to acknowledge Kerstin Roschitz, Bianca Mautner, Irmgard Windisch, Angela Wolfbauer, Sara Márcia Sardinha De Abreu Lobo, Jürgen Sallinger, Sanja Grahovac, Alexander Maaß, Lukas Fliri, Torsten Gutmann and Lukas Pachernegg, for their help with hand sheet forming, measurements, knowledge input and general support. Further, the authors acknowledge the support by TU Graz Open Access Publishing Fund.

Appendix A. Supplementary data

Supplementary data to this article can be found online at https://doi.org/10.1016/j.carbpol.2024.122354.

References

Ahankari, S., Lasrado, D., & Subramaniam, R. (2022). Advances in materials and fabrication of separators in supercapacitors. *Materials Advances, 3*, 1472–1496.

Andres, S., Appel, K. E., & Lampen, A. (2013). Toxicology, occurrence and risk characterisation of the chloropropanols in food: 2-monochloro-1,3-propanediol, 1,3-dichloro-2-propanol and 2,3-dichloro-1-propanol. *Food and Chemical Toxicology, 58*, 467–478.

Awada, H., Montplaisir, D., & Daneault, C. (2014). Cross-linking of papers based on thermomechanical pulp fibers by Polycarboxylic acids: Influence on the wet breaking length. *Industrial & Engineering Chemistry Research, 53*, 4312–4317.

Bhardwaj, N. K., Duong, T. D., & Nguyen, K. L. (2004). Pulp charge determination by different methods: Effect of beating/refining. *Colloids and Surfaces A: Physicochemical and Engineering Aspects, 236*, 39–44.

Caulfield, D. F. (1994). Ester crosslinking to improve wet performance of paper using multifunctional caboxylic acids, butanetetracarboxylic and citic acid. *Tappi Journal, 77*, 205–212.

Dufresne, A. (2013). Nanocellulose: A new ageless bionanomaterial. *Materials Today, 16*, 220–227.

Ehmann, H. M. A., Werzer, O., Pachmajer, S., Mohan, T., Amenitsch, H., Resel, R., … Spirk, S. (2015). Surface-sensitive approach to interpreting supramolecular rearrangements in cellulose by synchrotron grazing incidence small-angle X-ray scattering. *ACS Macro Letters, 4*, 713–716.

Fischer, W. J., Mayr, M., Spirk, S., Reishofer, D., Jagiello, L. A., Schmiedt, R., Colson, J., Zankel, A., & Bauer, W. (2017). Pulp fines-characterization, sheet formation, and comparison to microfibrillated cellulose. *Polymers (Basel), 9*.

Gericke, M., Amaral, A. J. R., Budtova, T., De Wever, P., Groth, T., Heinze, T., … Fardim, P. (2024). The European polysaccharide network of excellence (EPNOE) research roadmap 2040: Advanced strategies for exploiting the vast potential of polysaccharides as renewable bioresources. *Carbohydrate Polymers, 326, Article 121633*.

Greenhalgh, E. S., Nguyen, S., Valkova, M., Shirshova, N., Shaffer, M. S. P., & Kucernak, A. R. J. (2023). A critical review of structural supercapacitors and outlook on future research challenges. *Composites Science and Technology, 235, Article 109968*.

Häggkvist, M., Solberg, D., Wågberg, L., & Ödberg, L. (1998). The influence of two wet strength agents on pore size and swelling of pulp fibres and on tensile strength properties. *Nordic Pulp & Paper Research Journal, 13*, 292–298.

Hassan, E. A., Hassan, M. L., & Oksman, K. (2011). Improving bagasse pulp paper sheet properties with microfibrillated cellulose isolated from xylanase-treated bagasse. *Wood and Fiber Science, 43*, 76–82.

Hobisch, M. A., Phiri, J., Dou, J., Gane, P., Vuorinen, T., Bauer, W., … Spirk, S. (2020). Willow bark for sustainable energy storage systems. *Materials (Basel), 13*.

Hobisch, M. A., Zabler, S., Bardet, S. M., Zankel, A., Nypelo, T., Eckhart, R., … Spirk, S. (2021). How cellulose nanofibrils and cellulose microparticles impact paper strength-a visualization approach. *Carbohydrate Polymers, 254, Article 117406*.

Ji, B., Tang, P., Yan, K., & Sun, G. (2015). Catalytic actions of alkaline salts in reactions between 1,2,3,4-butanetetracarboxylic acid and cellulose: II. *Esterification. Carbohydrate Polymers, 132*, 228–236.

Ke, G., Xiao, Z., Jin, X., Yu, L., Li, J., & Zhang, H. (2020). Wrinkle recovery angle enhancement and tensile strength loss of 1,2,3,4-butanetetracarboxylic acid finished lyocell fabrics. *Textile Research Journal, 90*, 2097–2108.

Kes, M., & Christensen, B. E. (2013). A re-investigation of the mark-Houwink-Sakurada parameters for cellulose in Cuen: A study based on size-exclusion chromatography combined with multi-angle light scattering and viscometry. *Journal of Chromatography A, 1281*, 32–37.

Kokol, V., & Vivod, V. (2023). Cation-exchange performance of a citric-acid esterified cellulose nanofibrous membrane for highly-selective proteins' permeability and adsorption capacity. *Carbohydrate Polymers, 318*. Article 121134.

Kono, H., & Fujita, S. (2012). Biodegradable superabsorbent hydrogels derived from cellulose by esterification crosslinking with 1,2,3,4-butanetetracarboxylic dianhydride. *Carbohydrate Polymers, 87*, 2582–2588.

Korpela, A., Tanaka, A., & King, A. W. T. (2023). A comparative study of the effects of chemical crosslinking agents on NBSK handsheet properties. *BioResources, 18*, 937–948.

Kumaravel, V., Bartlett, J., & Pillai, S. C. (2020). Solid electrolytes for high-temperature stable batteries and supercapacitors. *Advanced Energy Materials, 11*.

Laheäär, A., Przygocki, P., Abbas, Q., & Béguin, F. (2015). Appropriate methods for evaluating the efficiency and capacitive behavior of different types of supercapacitors. *Electrochemistry Communications, 60*, 21–25.

Li, J., Jia, H., Ma, S., Xie, L., Wei, X.-X., Dai, L., … Chen, C.-M. (2023). Separator Design for High-Performance Supercapacitors: Requirements, challenges, strategies, and prospects. *ACS Energy Letters, 8*, 56–78.

Lund, K., & Brelid, H. (2014). 1,2,3,4-Butanetetracarboxylic acid cross-linked softwood Kraft pulp fibers for use in fluff pulp applications. *Journal of Engineered Fibers and Fabrics, 9*.

Ma, Y., Chen, K., Ma, J., Xu, G., Dong, S., Chen, B., Li, J., Chen, Z., Zhou, X., & Cui, G. (2019). A biomass based free radical scavenger binder endowing a compatible cathode interface for 5 V lithium-ion batteries. *Energy & Environmental Science, 12*, 273–280.

Ma, Y., You, X., Rissanen, M., Schlapp-Hackl, I., & Sixta, H. (2021). Sustainable cross-linking of man-made cellulosic fibers with poly(carboxylic acids) for fibrillation control. *ACS Sustainable Chemistry & Engineering, 9*, 16749–16756.

Quellmalz, A., & Mihranyan, A. (2015). Citric acid cross-linked Nanocellulose-based paper for size-exclusion Nanofiltration. *ACS Biomaterials Science & Engineering, 1*, 271–276.

Reishofer, D., Resel, R., Sattelkow, J., Fischer, W. J., Niegelhell, K., Mohan, T., … Spirk, S. (2022). Humidity response of cellulose thin films. *Biomacromolecules, 23*, 1148–1157.

Salmén, L., & Stevanic, J. S. (2018). Effect of drying conditions on cellulose microfibril aggregation and "hornification". *Cellulose, 25*, 6333–6344.

Šauperl, O., & Stana-Kleinschek, K. (2009). Differences between cotton and viscose fibers crosslinked with BTCA. *Textile Research Journal, 80*, 383–392.

Schlemmer, W., Selinger, J., Hobisch, M. A., & Spirk, S. (2021). Polysaccharides for sustainable energy storage - a review. *Carbohydrate Polymers, 265, Article 118063*.

Shallhorn, P., & Gurnagul, N. (2009). A simple model of the air permeability of paper. *In advances in pulp and paper research. Trans. Of the XIVth fund. Res. Symp. Oxford, 2009, (S.J. I'Anson, ed.), pp 475–490, FRC, Manchester, 2018*.

Siqueira, G., Bras, J., & Dufresne, A. (2010). Luffa cylindrica as a lignocellulosic source of fiber, microfibrillated cellulose, and cellulose nanocrystals. *BioResources, 5*, 727–740.

Song, Y., Zhao, G., Zhang, S., Xie, C., Yang, R., & Li, X. (2024). Chitosan nanofiber paper used as separator for high performance and sustainable lithium-ion batteries. *Carbohydrate Polymers, 329*, Article 121530.

Szubzda, B., Szmaja, A., Ozimek, M., & Mazurkiewicz, S. (2014). Polymer membranes as separators for supercapacitors. *Applied Physics A, 117*, 1801–1809.

Tammela, P., Olsson, H., Strømme, M., & Nyholm, L. (2014). The influence of electrode and separator thickness on the cell resistance of symmetric cellulose–polypyrrole-based electric energy storage devices. *Journal of Power Sources, 272*, 468–475.

Toigo, C., Singh, M., Gmeiner, B., Biso, M., & Pettinger, K.-H. (2020). A method to measure the swelling of water-soluble PVDF binder system and its electrochemical performance for Lithium ion batteries. *Journal of the Electrochemical Society, 167*.

Widsten, P., Dooley, N., Parr, R., Capricho, J., & Suckling, I. (2014). Citric acid crosslinking of paper products for improved high-humidity performance. *Carbohydrate Polymers, 101*, 998–1004.

Xu, D., Wang, B., Wang, Q., Gu, S., Li, W., Jin, J., … Wen, Z. (2018). High-strength internal cross-linking bacterial cellulose-network-based gel polymer electrolyte for dendrite-suppressing and high-rate Lithium batteries. *ACS Applied Materials & Interfaces, 10*, 17809–17819.

Yang, C. Q., Xu, Y., & Wang, D. (1996). FT-IR spectroscopy study of the Polycarboxylic acids used for paper wet strength improvement. *Industrial & Engineering Chemistry Research, 35*, 4037–4042.

Ye, T., Wang, B., Liu, J., Chen, J., & Yang, Y. (2015). Quantitative analysis of citric acid/sodium hypophosphite modified cotton by HPLC and conductometric titration. *Carbohydrate Polymers, 121*, 92–98.

Zaccagnini, P., Serrapede, M., Armandi, M., Bianco, S., Carminati, S., Zampato, M., … Lamberti, A. (2023). A high-temperature high-pressure supercapacitor based on ionic liquids for harsh environment applications. *Electrochimica Acta, 447*.

Zhang, H., Liu, J., Guan, M., Shang, Z., Sun, Y., Lu, Z., … Liu, H. (2018). Nanofibrillated cellulose (NFC) as a pore size mediator in the preparation of thermally resistant separators for Lithium ion batteries. *ACS Sustainable Chemistry & Engineering, 6*, 4838–4844.

Zhong, C., Deng, Y., Hu, W., Qiao, J., Zhang, L., & Zhang, J. (2015). A review of electrolyte materials and compositions for electrochemical supercapacitors. *Chemical Society Reviews, 44*, 7484–7539.

Zhou, Y. J., Luner, P., & Caluwe, P. (1995). Mechanism of crosslinking of papers with polyfunctional carboxylic acids. *Journal of Applied Polymer Science, 58*, 1523–1534.